Optimized norm-conserving pseudopotentials

1992 J. Phys.: Condens. Matter 4 7451

(http://iopscience.iop.org/0953-8984/4/36/018)

J. Phys.: Condens. Matter 4 (1992) 7451–7468. Printed in the UK

Optimized norm-conserving pseudopotentials

G Kresse†, J Hafner† and R J Needs‡

† Institut für Theoretische Physik, Technische Universität Wien, Wiedner Hauptstrasse 8–10, A-1040 Wien, Austria

‡ Theory of Condensed Matter Group, Cavendish Laboratory, University of Cambridge, Madingley Road, Cambridge CB3 0HE, UK

Abstract. In this paper we investigate the construction of norm-conserving 'soft-core' pseudopotentials with improved convergence properties of the plane-wave and perturbation expansions. The key factor is found to be the kinetic energy of the valence pseudo-orbitals. The total kinetic energy controls the convergence of the perturbation expansion of the total energy, the kinetic energy contained in the Fourier components beyond a certain cut-off limits the convergence of the plane-wave expansion. The simultaneous optimization of both expansions allows us to use the same pseudopotential in a rapidly convergent total-energy calculation for the crystalline phases, and in the calculation of interatomic forces to be used in atomistic simulations of the disordered phases.

1. Introduction

Electronic structure and total-energy calculations performed within the framework of the local-density approximation (LDA) [1] have demonstrated their ability to give reliable predictions of the physical properties of solids.

Mathematically, calculations of the electronic structure proceed by repeated diagonalization of the LDA-Hamiltonian on an arbitrary basis. Various basis sets such as plane waves, linearized augmented plane waves (LAPW), linearized muffin-tin orbitals (LMTO), Gaussians, and mixed basis sets have commonly been used. Both mathematically and numerically the plane-wave-basis formalism is very convenient to implement for both crystals and disordered materials. However, even with the development of diagonalization methods that can handle a basis of the order 10^4 plane waves [2–5], a plane wave expansion can be expected to converge only if the effect that the chemically inert core states exert on the valence states is replaced by an effective weak pseudopotential. These ideas date back to the early work of Fermi [6] and Hellmann [7] and have found widespread application since the seminal work of Phillips and Kleinman [8]. There is yet another reason for the interest in pseudopotentials. To date, the expansion in powers of the pseudopotential is the most natural way to break the total-energy into a sum of volume, pair, and many-atom contributions and to derive a set of volume, pair, and many-body forces for use in atomistic simulations of solids and liquids [9–12].

The only constraint on a pseudopotential is that it reproduces the valence electron spectrum, but has no bound states corresponding to the core electrons. An infinite number of pseudopotentials can be generated and much work has been carried out to determine the auxiliary conditions that give a pseudopotential that is accurate, transferable (in the sense that it adequately reproduces the all-electron behaviour

0953-8984/92/367451+18$04.50

outside the core region in different chemical environments), and computationally efficient.

In the sixties and seventies [9, 10], pseudopotentials were used mostly in perturbation calculations of the cohesive, structural, and dynamic properties. In this context, the Cohen–Heine criterion [13], which calls for a minimization of the kinetic energy of the pseudo-valence states $|\varphi\rangle$ via :

$$\delta\{\langle\varphi|T|\varphi\rangle/\langle\varphi|\varphi\rangle\} = 0 \tag{1}$$

leads to a very effective cancellation of the strong attractive crystal potential V by the repulsive part of the pseudopotential W and to an optimum convergence of the perturbation series. The Cohen–Heine criterion is implemented most effectively within the framework of pseudopotentials constructed via an orthogonalized plane-wave (OPW) expansion of the valence states [14]. OPW pseudopotentials are constructed (and optimized) for ions in an electron gas of the density corresponding to the element, alloy or compound under consideration [15]. The fact that no specific reference configuration has to be assumed for the generation of the pseudopotential ensures that there is no problem of 'transferability'. The optimization improves the convergence of the perturbation series, but not necessarily the convergence of the plane-wave expansion. In fact, it turns out that due to the 'hard core' character of OPW pseudopotentials, plane-wave convergence is rather slow so that these potentials are not very well suited for non-perturbative total energy calculations.

This has led to the construction of 'soft-core' pseudopotentials of various types [16–20]. Nodeless pseudo-orbitals are constructed for atomic reference configurations in such a way that the valence all-electron and pseudopotential eigenvalues are equal and that the inversion of the radial Schrödinger equation produces a smooth, 'soft-core' pseudopotential (where smoothness is considered to be synonymous with a rapid convergence of the calculated total-energy with respect to an increase in the size of the plane-wave basis set). The pseudopotential should reproduce the results of all-electron calculations in different environments as closely as possible, i.e. it should be transferable. An initial test of the transferability is provided by the logarithmic derivatives of the radial pseudo- and all-electron wavefunctions w_l^{PP} and w_l^{AE} at the radius R_{cl} beyond which w_l^{PP} and w_l^{AE} are identical. Evidently this requires the equality of the logarithmic derivatives, i.e. :

$$\frac{1}{w_l^{PP}(r,E)}\frac{\mathrm{d}w_l^{PP}(r,E)}{\mathrm{d}r}\bigg|_{r=R_{cl}} = \frac{1}{w_l^{AE}(r,E)}\frac{\mathrm{d}w_l^{AE}(r,E)}{\mathrm{d}r}\bigg|_{r=R_{cl}} . \tag{2}$$

By construction, equation (2) holds for the energy-eigenvalue E_l. For a transferable pseudopotential, equation (2) should hold for a range of energies around E_l. An identity similar to the Friedel sum rule relates the energy derivative of the logarithmic derivatives at $r = R_{cl}$ to the angular-momentum component of the charge within that sphere [21, 22]

$$-\frac{\partial}{\partial E}\frac{\partial}{\partial r}\ln w_e(r,E)\bigg|_{r=R_{cl}} = \frac{1}{w_e^2(R_{cl},E)R_{cl}^2}\int_0^{R_{cl}} w_e^2(r,E)r^2\,\mathrm{d}r . \tag{3}$$

Equation (3) shows that if the transformation from the all-electron orbitals to the pseudopotentials conserves the norm of the wavefunction, then the norm-conserving

pseudopotential can also be expected to be transferable. Evidently extensions of this concept involve the adjustment of the reference energy (even at the expense of using unbound wavefunctions [23]) or equating higher-order energy derivatives [24] of (2).

However, there is one drawback in the original norm-conserving pseudopotentials [25]: the pseudopotential matrix element is large for momentum transfers around $q = 2k_F$ (figure 1). Therefore, although the plane-wave convergence is good, the convergence of the perturbation series is slow and effective interatomic forces calculated in a low-order perturbation approximation are unrealistic. Hence it is not possible to switch between a perturbation calculation and iterative total-energy calculations, and the decomposition of the total-energy into volume, pair, and many-body forces cannot be used to analyse the results in terms of interatomic interactions.

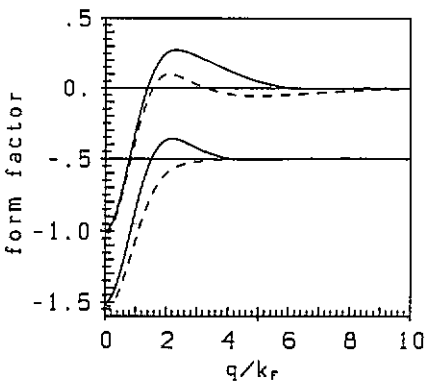

Figure 1. Screened pseudopotential matrix element $\langle k+q|w|k\rangle$ for Al, calculated using the optimized orthogonalized plane-wave pseudopotential (dashed line) and using the norm-conserving Bachelet–Hamann–Schlüter (BHS) pseudopotential (full line). The upper part contains the on-Fermi-sphere ($|k| = |k+q| = k_F$) matrix element for $q \leqslant 2k_F$ and the back-scattering matrix element $(-q||(q+k))$ for $q > 2k_F$, the lower part shows the matrix element for forward scattering.

In this paper we report on an attempt to optimize simultaneously the plane-wave convergence and the convergence of a perturbation expansion for the total-energy. We show that by exploiting the improved schemes for constructing norm-conserving pseudopotentials it is possible to obtain a low cut-off energy for the plane wave expansion and realistic atomic forces that can serve for atomistic simulations of disordered phases.

2. Optimizing norm-conserving pseudopotentials

Norm-conserving pseudopotentials are constructed in such a way that the logarithmic derivatives of the wavefunction and the pseudo-wavefunction and the energy derivative of the logarithmic derivatives agree at a certain cut-off radius R_{cl}. The second condition guarantees the conservation of the norm (see equations (2) and (3)). This leaves considerable freedom in the construction of the pseudopotential. Many of the early norm-conserving pseudopotentials [26,27] are of the hard-core type (i.e. having a repulsive r^{-2} divergence at the origin). This leads to a q^{-1} decay in the reciprocal space, and hence to very poor convergence property. The Hamann–Schlüter–Chiang (HSC) method [17,18] begins with a self-consistent all-electron calculation for an atomic reference configuration. Then, the full potential $V^{AE}(r)$ is subjected to a cut-off in the core region:

$$V_l^1(r) = V^{AE}(r)\left(1 - f^1(r/R_{cl})\right) \ . \tag{4}$$

In the second step, the constant c_l in the ansatz

$$V_l^2(r) = V_l^1(r) + c_l f^2(r/R_{cl}) \tag{5}$$

is chosen so that the nodeless radial eigenfunction $w_l^2(r)$ belonging to $V_l^2(r)$ has the correct reference energy ϵ_l. Third, the constants γ_l and δ_l are determined so that the pseudo-wavefunction $w_l^3(r)$ is normalized and identical to the all-electron solution for $r > R_{cl}$:

$$w_l^3(r) = \gamma_l \left(w_l^2(r) + \delta_l r^{l+1} f^3(r/R_{cl})\right) . \tag{6}$$

In the HSC method the functions f^1, f^2, f^3 are chosen to be identical. Vanderbilt (VAN) [20] noted that the freedom to choose different f^i may be exploited in such a way that the resulting pseudopotentials decay much faster in reciprocal space than the HSC potentials. This improves the plane-wave convergence slightly, with no loss of transferability.

Shirley *et al* (SAMJ) [24] introduced the concept of extended norm-conserving pseudopotentials. Extended norm conservation means that the correctness of the radial logarithmic derivative is extended to higher order in energy: the envelope function $f^3(r/R_{cl})$ (see equation (6)) is chosen such that $\partial x/\partial E$ and $\partial^2 x/\partial^2 E$ (where x is the logarithmic derivative defined in (2)) match simultaneously at $r = R_{cl}$. This leads to a marginal improvement of transferability, but to a somewhat slower decay of the pseudopotential in reciprocal space.

Rappe *et al* (RRJK) [28] noted that a good convergence of the total-energy can be achieved when the higher Fourier components of the pseudo-wavefunction contain very little kinetic energy. This is in essence the Cohen–Heine criterion (1), but more specifically: according to this criterion, the kinetic energy is minimized, but no control is exercised on the distribution of the kinetic energies. Optimal convergence of the plane-wave expansion is obtained when the kinetic energy contained in the high Fourier components of the pseudo-wavefunction is minimized directly. This is achieved by augmenting $w_l^{PS}(r)$ for $r < R_{cl}$ by a function $C_l(r)$. $C_l(r)$ is chosen such that the logarithmic derivative of the optimized pseudo-wavefunction $\tilde{w}_l^{PP}(r) = w_l^{PP}(r) + C_l(r)$ and its energy derivative match the all-electron solution at $r = R_{cl}$ and that the kinetic energy beyond a momentum cut-off q_c is minimized. If φ_l is the pseudo-wavefunction whose radial part is $\tilde{w}_l^{PP}(r)$, this requires minimizing

$$-\int \mathrm{d}^3 r \varphi_l^*(r) \Delta \varphi_l(r) - \int_0^{q_c} \mathrm{d}^3 q \; q^2 \varphi_l^*(q) \varphi_l(q) . \tag{7}$$

The contribution to the kinetic energy by plane waves with $q > q_c$ is a direct measure of the level of convergence achieved for the total-energy. The RRKJ scheme allows one to construct pseudopotentials with very good convergence of the total-energy, the choice of the cut-offs q_c and R_{cl} effectively controls the rate of convergence, and the accuracy that can be achieved with a given pseudopotential.

Trouiller and Martins (TM) [29] started from an analysis of the correlations between the asymptotic form of the pseudopotential in q-space and the discontinuities in the derivatives of the pseudo-wavefunctions at $r = R_{cl}$. They proposed to improve the smoothness of the pseudopotential by imposing (beyond norm conservation) (i) the continuity of the pseudo-wavefunction and its first four derivatives at $r = R_{cl}$, and

(ii) zero curvature of the screened pseudopotential at the origin. The TM pseudopotentials allow for larger cut-off radii than the other pseudopotentials, at comparable transferability. The larger cut-off, together with the zero curvature at the origin, greatly improves the plane-wave convergence of total-energy calculation.

Very recently Vanderbilt [30] (VAN2) proposed a generalized norm-conservation criterion for non-local pseudopotentials of the Kleinman–Bylander [31] form. The idea is to transform w_l^{AE} into a w_l^{PP} for each l independently, and to match the correct scattering properties at different energies spanning the band width of the target phase. The new pseudopotential has a formal resemblance to the Phillips–Kleinman pseudopotential. The main advantage of this pseudopotential is that it also allows for the successful pseudization of orbitals that cannot conveniently be pseudized by conventional techniques, e.g. 2p orbitals of the first row elements [30, 32].

All these schemes lead to a common conclusion: by imposing additional conditions beyond norm-conservation, it is possible to improve plane-wave convergence without compromising transferability. Both the convergence and the transferability depend mainly on the cut-off radii. Note, however, that the cut-offs are defined in different ways: RRKJ and TM match the wavefunctions at R_{cl}, whereas in the HSC and VAN schemes, R_{cl} is the characteristic distance of a cut-off function varying steeply around R_{cl}, so that the wavefunctions match only at distances that are considerably larger (typically by fifty per cent) than R_{cl}. Quite generally, a larger cut-off radius leads to better plane-wave convergence. In the following we shall test the transferability, the plane-wave convergence, and the convergence of the perturbation expansion in the different pseudopotential schemes. We shall restrict our discussion to the (s,p)-bonded elements, since it cannot be expected that perturbation theory works for d metals, even after optimization of the pseudopotentials

3. Transferability

The most straigthforward way to test the transferability of a pseudopotential is through the calculation of the phase-shifts and of the energies of excited one-electron levels of atomic systems. Figure 2 shows the $l = 0$ and $l = 1$ phase shifts at a distance of r=3.6 au for Al calculated using BHS and RRKJ pseudopotentials and different values for the cut-off radii. The reference configuration is $3s^2\,3p^1$. The RRKJ pseudopotential was optimized for a convergence of 1 mRyd. This means that for each cut-off R_{cl} the parameter q_{cl} was chosen such that the kinetic energy beyond this cut-off was less than 1 mRyd. The phase shifts of the VAN and TM pseudopotential depend in a very similar way on the cut-off.

A standard value for the cut-off radius that guarantees that the pseudo- and all-electron wavefunctions are identical over the entire range of interest would be R_{cl} = 1.2 au in the VAN scheme. However, we find that it is safe to increase R_{cl} by more than fifty per cent without seriously affecting the phase-shifts in the range $\pm$ 0.5 Ryd around the atomic reference eigenvalues.

The same conclusion may be drawn from the calculated excitation energies. Table 1 lists the errors in the pseudopotential predictions for the energy of the 4s state of Al, relative to an all-electron frozen-potential calculation. We find that the pseudopotential error increases with larger cut-offs, but remains below 1 mRyd except for extremely large cut-off radii. As we have already emphasized above, the numerical values of the cut-off radii are not directly comparable. What we want to compare

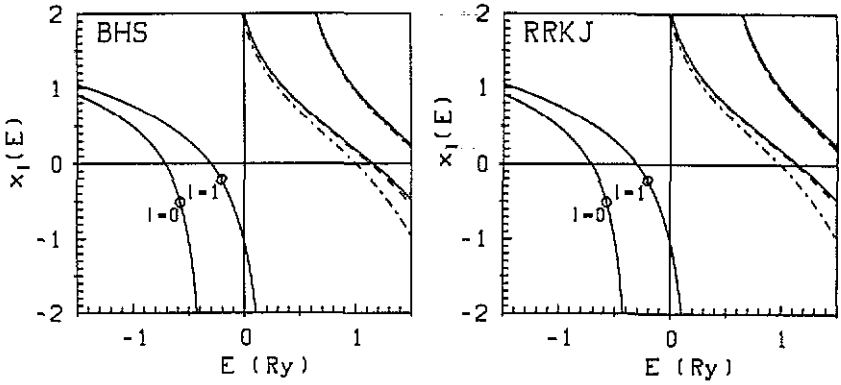

Figure 2. Phase-shifts $x_l(E)$ (l=0,1) for Al, calculated using the BHS and RRKJ pseudopotentials and different cut-off radii ($R_{c0} = R_{c1}$). (*a*) BHS: dashed line R_{cl}=1.2 au, dashed-dotted R_{cl}=1.6 au; (*b*) RRKJ: dashed line R_{cl}=1.8 au, dashed-dotted R_{cl}=2.6 au. The full line shows the exact phase shifts from the all-electron calculations. The open circles mark the atomic reference energies.

are pseudopotentials which can be expected to have a similar rate of convergence in plane-wave convergence. A good measure of the rate of convergence is the kinetic energy $E_{kin}(q > q_c)$ contained in the high-momentum components of the valence-electron wavefunctions (cf equation (7)). If we set a tolerance level on the plane wave convergence by requiring $E_{kin}(q > q_c)$ to be smaller than a certain value, this fixes a plane-wave cut-off energy $E_{cut} = q_c^2$. These cut-off energies are given in table 1. For all types of pseudopotentials, the cut-off energy necessary to achieve convergence within 1 mRyd decreases with increasing R_{cl}. With E_{cut} = 8 Ryd, convergence within this level is obtained with R_{cl} = 1.6 au (HSC), R_{cl} = 1.8 au (VAN), R_{cl} = 2.6 au (RRKJ), and R_{cl} = 2.8 au (TM). With these cut-off radii, the pseudopotential error in the excitation energy is 0.001 ± 0.0002 Ryd.

In addition table 1 contains the total kinetic energy. All calculations performed by us (see also section 4) show that the kinetic energy is indeed a very good indicator of the convergence of the perturbation expansion.

This shows that for all pseudopotential schemes, there is a trade-off between transferability, plane-wave convergence, and convergence of the perturbation calculation. All schemes proposed in the literature are essentially equivalent, at least for states with an angular momentum quantum number l that is also present in the core. If this is not the case (such as for 2p and 3d valence orbitals), the more sophisticated algorithms of RRKJ and TM are to be preferred, because they control the kinetic energy in the high Fourier components more efficently than the simples schemes of BHS and VAN.

4. Plane-wave convergence

The convergence criterion that we used in the last section is only a qualitative one, ultimately convergence has to be checked in a total-energy calculation. An initial hint is given by the form of the pseudopotential in real space (figure 3) and in Fourier space (figure 4). Quite generally, an increase in the cut-off radii reduces the curvature of the pseudopotentials close to the origin and leads to a reduced

Table 1. Errors ΔE produced by various pseudopotentials for the one-electron excitation energy of the 4s electron, together with the kinetic energy E_{kin} of the s pseudo-wavefunction and the cut-off energy E_{cut} necessary to achieve convergence of a plane-wave expansion of the s pseudo-wavefunction within 1 mRyd (0.1 mRyd). Energies are given in Ryd.

R_{cl} (au)	ΔE	E_{cut}	E_{kin}
Vanderbilt (VAN)			
1.2	0.00009	13.3 (30.57)	0.377
1.5	0.00033	10.3 (20.47)	0.348
1.8	0.00102	8.0 (10.27)	0.325
2.1	0.00200	6.3 (8.35)	0.315
Rappe *et al* (RRKJ)			
1.8	0.00010	12.8 (43.5)	0.375
2.3	0.00029	9.8 (34.1)	0.344
2.6	0.00079	8.3 (27.8)	0.323
2.8	0.00140	6.6 (24.0)	0.315
Troullier and Martins (TM)			
1.8	0.00010	22.8 (32.7)	0.370
2.4	0.00026	17.7 (25.3)	0.347
2.8	0.00087	8.7 (18.8)	0.327
3.4	0.00200	5.7 (12.0)	0.313
Hamann, Schlüter and Chiang (HSC)			
1.2	0.00010	18.2 (30.6)	0.371
1.4	0.00029	10.6 (23.4)	0.346
1.6	0.00077	7.9 (17.7)	0.325
1.8	0.00163	6.3 (12.8)	0.315

non-locality. In Fourier space this is reflected by reduced Fourier components at intermediate ($q \approx 2k_F$) and at large momentum transfers. This reduction is strongest for $q \geqslant 2k_F$, i.e. for momentum transfers close to the shortest reciprocal lattice vectors in a close-packed structure. Thus we can expect that an increase in the cut-off radius improves the convergence of a perturbation calculation of the total-energy. However, we want to improve simultaneously the convergence of the plane wave expansion and this is not immediately related to the damping of the high-q oscillations alone. We discuss plane-wave convergence first. Figure 5 shows the total-energy for face-centred cubic Al, calculated self-consistently for the VAN and TM pseudopotentials using different cut-off energies and cut-off radii. All calculations are based on a $(8 \times 8 \times 8)$ grid of special k-points [33] in the first Brillouin zone. The pseudopotential was generated for an $3s3p^2$ reference configuration and the exchange-correlation potential of Ceperley and Alder [34] was used. For both types of potentials an increase in the cut-off radius yields a marked improvement in the convergence of the calculated total-energy. For the VAN pseudopotential and $R_{cl}=1.8$ au, the total energy is converged to within 0.1 mRyd with a cut-off energy of $E_{cut} = 10$ Ryd. For a cut-off radius of $R_{cl}=1.2$ au the same accuracy requires a much larger cut-off of at least 16 Ryd.

The variation in the calculated bulk properties with the cut-off radius at fixed cut-off energy (which must be large enough to achieve reasonable convergence even

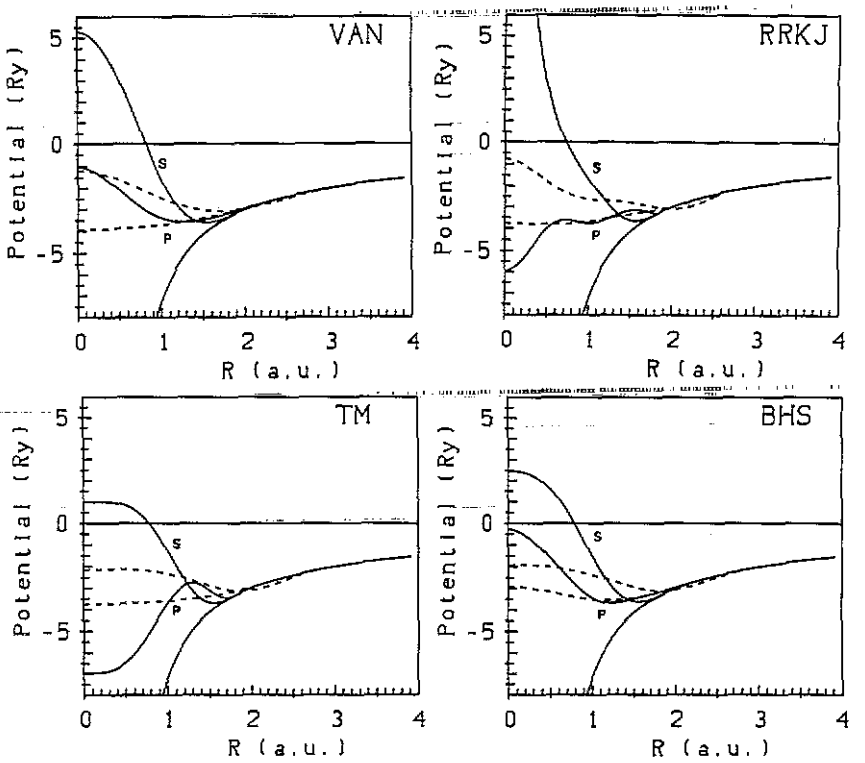

Figure 3. The ionic pseudopotentials for Al in real space, generated using four different pseudopotential schemes and different cut-off radii ($R_{c0} = R_{cl}$): (*a*) VAN: full line R_{cl}=1.2 au, dashed line R_{cl}=1.8 au; (*b*) RRKJ: full line R_{cl}=1.8 au, dashed line R_{cl}=2.6 au; (*c*) TM: full line R_{cl}=1.8 au, dashed line R_{cl}=2.8 au; (*d*) BHS: full line R_{cl}=1.2 au, dashed line R_{cl}=1.6 au.

for the smallest R_{cl}) is again a measure of the transferability. Table 2 summarizes the results for the binding energy, equilibrium atomic volume and bulk modulus of Al, calculated self consistently using the VAN pseudopotential and different cut-off radii. In all calculations a cut-off energy of 16 Ryd and a grid of $(8 \times 8 \times 8)$ special points has been used. A lowering of the cut-off to 8 Ryd influences essentially only the bulk modulus. We find that at least for $R_{cl} \leqslant 1.8$ au the variation in the total-energy is < 0.5 per cent, even the variation of the bulk modulus (calculated by fitting Murnaghan's equation of state to the calculated energies) is $\leqslant 10\%$. An even more stringent test of the pseudopotentials is provided by the calculation of vibrational eigenfrequencies using the 'frozen-phonon approach', i.e. by taking the difference in total-energy between the ideal lattice and a distorted lattice with displacement pattern characteristic of the eigenmodes at a high symetry k-point. The calculations have been performed with a plane-wave cut-off energy of 16 Ryd and 8 Ryd and a $(12\times12\times12)$ mesh of special k-points. The phonon frequencies have been determined from the variation of the energy with the amplitude of the displacement and by using the force theorem [37]. Again we find that, on varying R_{cl} between 1.2 au and 2.0 au the longitudinal frequency varies by only 2 per cent, in the tranverse eigenmode the change is about 3% (table 3). About the same order of uncertainty arises from the Brillouin-zone sampling. Due to the very complicated Fermi surface of Al, a very fine k-mesh is required and with a $(12 \times 12 \times 12)$ mesh the estimated error is of the

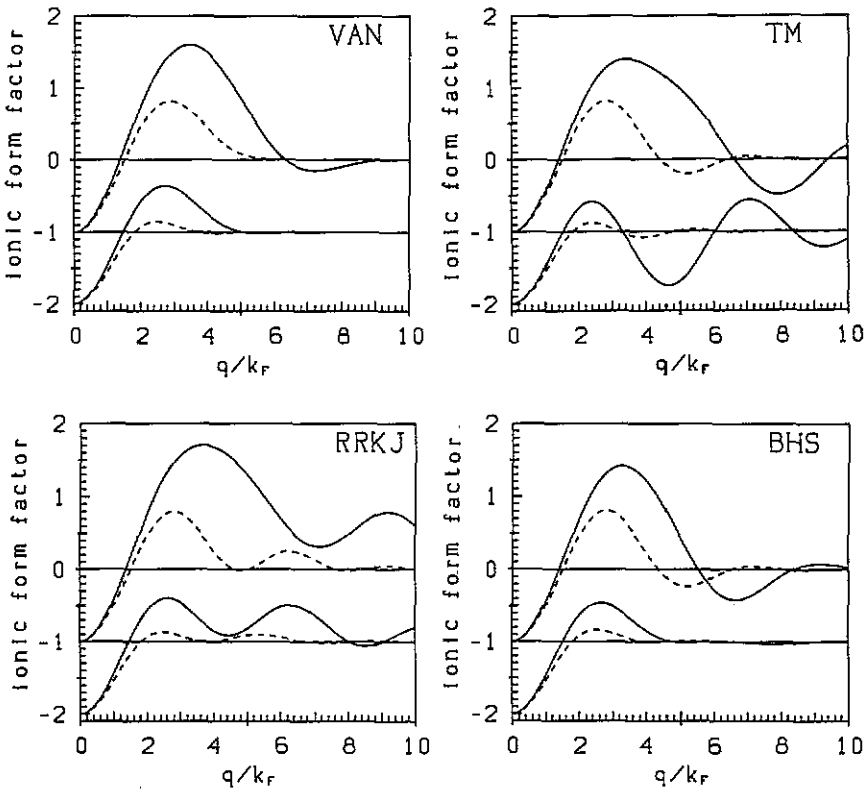

Figure 4. The form factor $q^2/(8\pi Z)(k+q|w|k)$ of the ionic potential for Al, for backward- (upper part) and forward-scattering (lower part), as calculated using the four different pseudopotential schemes: For definitions of the symbols see figure 3.

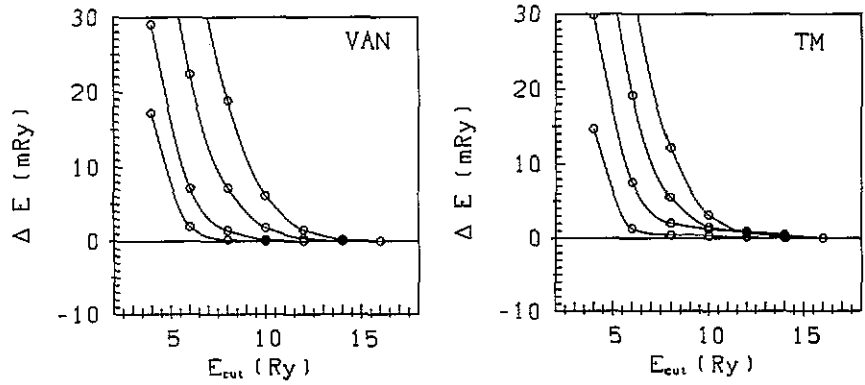

Figure 5. The calculated total energy ΔE of face-centred cubic aluminium calculated using the VAN and TM pseudopotentials and different cut-off radii versus the cut-off energy E_{cut} of the plane wave basis set. The zero of energy for each curve is the total energy calculated for a cut-off energy of 16 Ryd. (*a*) VAN: R_{cl} = 1.2, 1.5, 1.8, 2.1 au; (*b*) TM: R_{cl} = 1.8, 2.4, 2.8, 3.4 au.

order of a few per cent in the eigenfrequencies. Thus again we conclude that it is safe to extend the cut-off radius to about 1.8 au since the slight loss in transferability

Table 2. Binding energy E_B, equilibrium atomic volume V_a, and bulk modulus B for FCC Al calculated using the Vanderbilt pseudopotential and different cut-off radii. The results were obtained from self-consistent calculations and a cut-off of 8 Ryd (SC 8) and 16 Ryd (SC 16) and using second- and third-order perturbation theory (2-PT, 3-PT). The experimental values and the results of the pseudopotential calculations of Lam and Cohen [35] are given for comparison.

R_{cl} (au)	1.2	1.6	1.8	2.0
SC 8				
E_B (Ry at.)	−4.165	−4.174	−4.190	−4.209
V_a (au)	117.1	115.9	113.4	112.2
B (kBar)	884	886	839	867
SC 16				
E_B (Ry at.)	−4.167	−4.178	−4.191	−4.209
V_a (au)	117.4	116.3	114.5	112.2
B (kBar)	775	790	812	857
2-PT				
E_B (Ry at.)		−4.221	−4.200	−4.208
V_a (au)		91.9	103.5	108.9
B (kBar)		1040	726	641
3-PT				
EB (Ry at.)	−4.069	−4.175	−4.188	−4.204
V_a (au)	137.8	111.9	112.6	112.5
B (kBar)	406	646	636	629

	Experiment	Lam and Cohen
V_a (au)	109.6	108.7
B (kBar)	722	715

is outweighed by the improved convergence properties.

5. Convergence of the perturbation series

We now turn to the investigation of the convergence of the perturbation series. The general form of the Rayleigh–Schrödinger expansion of the electronic ground-state energy is given by [38]

$$E = E_0 + E_1 + E_2 + E_3 + \dots \tag{8}$$

with

$$E_k = V_a \sum_{q_1,\dots,q_k} \Gamma^{(k)}(q_1,\dots,q_k)\; w(q_1)\dots w(q_k)\; S(q_1)\dots S(q_k).$$

Here $S(q)$ is the geometric structure factor describing the spatial arrangement of the ions. For simplicity eq. (8) has been formulated for a local pseudopotential. Explicit expressions for the first- and second-order terms for non-local pseudopotentials are given in [9] and [10], the third-order contribution for non-local potentials has been

Table 3. Phonon frequencies ω (in 10^{13} rad sec^{-1}) for face-centred cubic Al at $q = (100)(2\pi/a)$, calculated using the 'frozen-phonon' approach with a variable plane-wave cut-off of 8 and 16 Ryd (SC8, SC16) and second- and third-order perturbation theory (2-PT, 3-PT). The Vanderbilt pseudopotential with a variable cut-off R_{cl} has been used. The experimental values are given for comparison (measured at 80 K by Stedman and Nilsson [36]).

R_{cl} (au)	1.2	1.6	1.8	2.0	Experiment
SC 8					
ω_T	3.252	3.220	3.272	3.364	3.65
ω_L	6.488	6.331	6.277	6.250	6.08
SC 16					
ω_T	3.290	3.288	3.308	3.384	
ω_L	6.332	6.286	6.238	6.222	
2-PT					
ω_T	4.075	3.811	3.839	3.778	
ω_L	6.962	6.342	6.238	6.176	
3-PT					
ω_T	4.521	3.791	3.770	3.757	
ω_L	6.823	6.281	6.201	6.175	

discussed by McLaren [39]. The 'multipole functions' $\Gamma^{(k)}(q_1, \ldots, q_k)$ are general characteristics of the electron gas. $\Gamma^{(2)}(q, -q)$ may be expressed in terms of the susceptility $\chi(q)$ of the electron gas in the random-phase approximation and the local-field corrections $G(q)$ accounting for the exchange and correlation interactions between the electrons [9, 10]. Explicit expressions for higher order multipole functions are given in [40–42].

Various approximations have been proposed for the local-field corrections. Using local density functional theory, one obtains $G(q) = \gamma(q/k_F)^2$ with the coefficient γ determined by the compressibility sum rule for the electron gas [43, 44]. It has been shown that the LDA local-field corrections lead to realistic predictions, and we decided to use this form for $G(q)$ with γ calculated according to the Ceperley–Alder parametrization of the exchange–correlation functional used in the calculation of the ionic pseudopotential. However, further sum rules relate $G(q)$ to the correlation energy, the electron–electron pair correlation function etc. The Ichimaru–Utsumi (IU) local field is consistent with the Ceperley–Alder exchange and correlation (at least in the limit $q \to 0$) and satisfies all relevant sum rules.

While the second-order terms can be calculated for the full non-local form of the pseudopotential, the third-order terms can be computed only in a local approximation. It was shown [46] that the so-called 'on-Fermi-sphere' approximation ($|k| = k_F$ and $|k+q| = k_F$ for $q \leqslant 2k_F$ and $-q \| (q+k)$ for $q > 2k_F$) for the pseudopotential form factor leads to an overestimate of the third-order contribution. Following Bertoni *et al* [46, 47] we constructed a local pseudopotential form factor by averaging $\langle k|w|k+q\rangle$, weighted with the free electron energy denominator $(k^2 - |k+q|^2)^{-1}$, over all possible directions of k for a given value of q. This 'semi-local' form factor has been used in calculations of the third-order contributions to the total-energy and to phonon frequencies. Explicit expressions for the third-order contribution to the dynamical matrix are given in Kagan and Brovman [48].

The perturbation results for the static properties of Al, calculated with the VAN pseudopotential and different cut-off radii are listed in table 2. For small cut-off

radii, perturbation theory gives very bad results, especially for the equilibrium volume. An increase in the cut-off radius substantially improves the convergence of the perturbation series, together with the plane-wave convergence. For $R_{cl} \approx 1.8$–2.0 the perturbation theory is rather well converged even at second order, with small third-order corrections. The same conclusion may be drawn from calculations of the phonon frequencies (table 3): on increasing the cut-off radius, the higher-order ($n \geqslant 3$) perturbation contributions to the eigenfrequences are quickly reduced and the results are in reasonable agreement with the 'frozen-phonon' values. Perturbation theory allows one to calculate phonon frequencies over the entire Brillouin zone. An example is shown in figure 6. We see that with a suitable choice of the cut-off radius, the third-order contributions are rather small, except for transverse phonons in the [100] and [111] directions. The possibilty of performing 'frozen-phonon' and perturbation calculations with the same pseudopotential allows us for the first time, to assess the accuracy of the predictions of lattice dynamical properties using perturbation theory. This point will be elaborated in more detail in another paper [49].

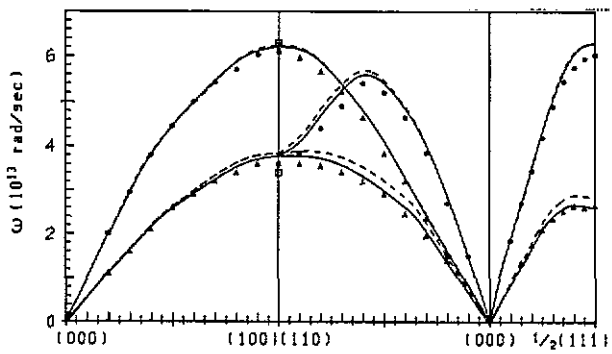

Figure 6. Phonon-dispersion relations for face-centred cubic Al in 10^{13} rad sec^{-1}, calculated using the VAN pseudoptotential with a cut-off radius of $R_{cl}=1.8$ au and the LDA local field corrections. Broken lines second-order, full lines third-order perturbation theory. The open squares represent the 'frozen-phonon' frequencies from a selfconsistent total-energy calculation. The circles and triangles mark the experimental results of Stedman and Nilsson [36].

The phonon frequencies depend slightly on the local field corrections. Using the IU form instead of the LDA local field correction changes the phonon frequencies by about 2 per cent.

6. Interatomic forces

To second-order in the pseudopotential, the total-energy may be written as the sum of a volume energy (representing the electron gas terms plus the self-energy of the pseudoatom) and a pair-interaction term [9, 10]. Higher-order terms of order n contribute an n-body term and corrections to the volume and all m-body interactions with $m < n$. The characteristic form of the density-dependent pair potentials is determined by a screened short-range repulsion and long-range Friedel-oscillations arising from the rapid variation of the Fermi occupation function around E_F. The amplitude of the Friedel oscillations is set by the on-Fermi-sphere matrix element of

arising from the rapid variation of the Fermi occupation function around E_F. The amplitude of the Friedel oscillations is set by the on-Fermi-sphere matrix element of the pseudopotential [50,51]. It has been shown that the variation of the effective pair potential with electron density and pseudopotential explains the trends in the crystalline [50] and liquid [52–55] structures of the elements.

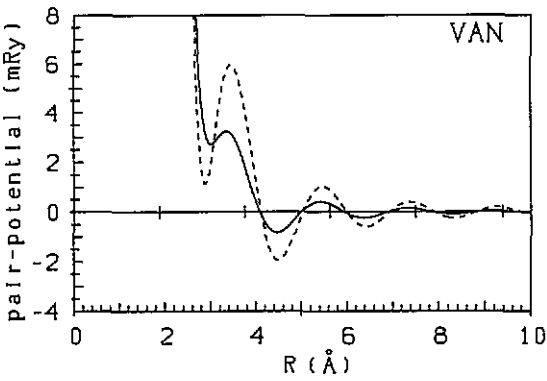

Figure 7. Effective pair potential $\Phi(R)$ for Al, calculated using the Vanderbilt pseudopotential and the LDA local-field correction. Broken curve $R_{cl}=1.2$ au, full curve $R_{cl}=1.8$ au.

As the $q = 2k_F$ matrix element of the pseudopotential depends strongly on the cut-off radius, we expect a strong variation of the pair potential $\Phi(R)$ with R_{cl}. This is demonstrated for the VAN pseudopotential in figure 7: the cut-off radius influences the amplitude, but not the phase of the oscillations. The influence is strongest around the nearest-neighbour distance. The most direct way to analyse the accuracy of the pair potential is via a molecular dynamics simulation of the liquid structure. The pseudopotential with the smallest cut-off radius (and hence the largest matrix element at $q = 2k_F$) produces the deepest local minimum around the nearest-neighbour distance in $\Phi(R)$, see figures 7 and 2. It leads to a glassy rather than a liquid structure for temperatures close to the melting point (after cooling from higher temperatures). A pseudopotential with a larger cut-off (and hence optimal convergence of the perturbation series) leads to an almost perfect agreement of the calculated static structure factor with experiment (figure 8). This shows that the optimization of the perturbation series is also very effective in folding down higher-order contributions to the pair forces.

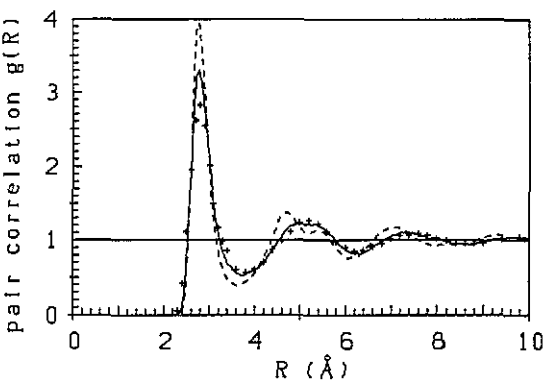

Figure 8. Pair correlation function $g(R)$ for liquid Al at 953 K, calculated using molecular dynamics and the pair potentials shown in figure 7. The crosses show the experimental values for $g(R)$ (after Waseda [53]).

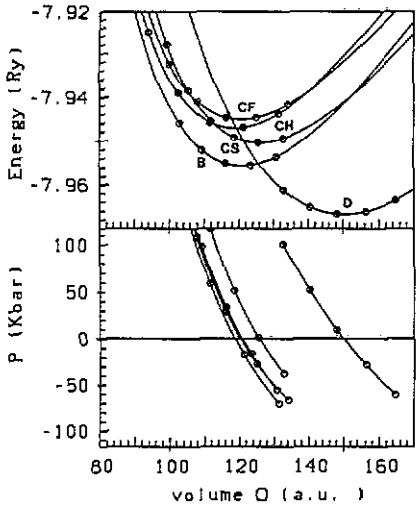

Figure 9. Total energy (upper panel) and pressure (lower panel) of Ge in the diamond (D), β-tin (B), face-centred cubic (CF), simple cubic (CS) and hexagonal close-packed (CH) structures, as a function of volume calculated with the VAN pseudopotential (cf text).

The proper decomposition of the total-energy into volume, pair and many-body contributions is very important for understanding the physical mechanism responsible for stabilizing the open structures of the metallic, semi-metallic and semiconducting B-group elements. Recent work based on OPW and empirical pseudopotentials [55–59] has shown that the interplay of the volume and pair forces alone explains the trend form high to low coordination numbers with increasing electron density, although pair forces alone are not sufficent to stabilize the low-coordinated crystalline structures. In the liquid phase, on the other hand, volume and pair forces alone yield an accurate description of the pair correlation functions of the molten elements from groups III to VI [55–59]. Significant differences between the pair-potential approach and full many-body calculations within a local-density molecular dynamics framework [2, 60, 61] appear only at the level of four-atom correlations. Here we want to verify that a calculation on the basis of optimized 'soft-core' pseudopotentials leads to the same conclusion. The example chosen is Ge. Good convergence properties are achieved by using the largest cut-off radii R_{cl} compatible with a correct form of the pseudo-orbitals in the bonding region. For a B-group element like Ge we have to consider the different spatial variation of the highest core orbitals: the 4s and 4p wavefunctions are more localized than the 3d wavefunction, and this influences the form of the s, p and d components of the valence pseudo-orbitals. We find that the s and p cut-off radii are restricted to $R_{cs,cp} \leqslant 1.3$ au, whereas for the d-cut-off radius a large value $R_{cl} \approx 1.8$ au is allowed. Figure 9 shows the total-energy and pressure of Ge in the diamond, β-tin, face-centred cubic, simple cubic and hexagonal close-packed structures, as a function of volume calculated with a Vanderbilt pseudopotential and $R_{cs} = R_{cp} = 1.2$, $R_{cd} = 1.8$ au. The calculated structural energy differences and the transition pressure for diamond to β-tin are in good agreement with the results of Chang and Cohen [62]. Figure 10 shows the pair interaction in liquid Ge just above melting point, calculated using the same pseudopotential, figure 11 the molecular dynamics results for the pair-correlation function in the melt. Although the pair-correlation function is in good agreement with experiment, it is interesting to explore the influence of many-body forces. A calculation of the explicit real-space

form of the three-body interactions via a six-dimensional Fourier transform of the third order perturbation characteristic in k-space (see [10], section 2.2 for details) is impracticable. However, it is possible, at least for small ensembles, to calculate the third-order contributions to the pair and triplet forces in a k-space formalism and to use these forces in a molecular dynamics simulation [63]. The dashed line in figure 11 shows the influence of the third-order contributions. We find that as expected, third-order contributions are small for a potential with optimized convergence properties. Note, however, that because of the use of the electron-gas response function, the three-body forces used in these calculations are correct only for the metallic liquid phase, and not for the semiconducting crystalline phase.

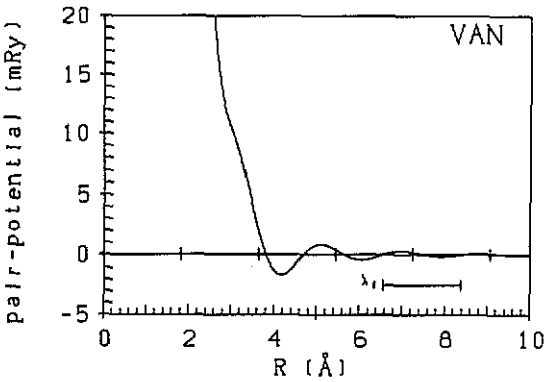

Figure 10. Effective pair potential $\Phi(R)$ for Ge, calculated using the Vanderbilt pseudopotential.

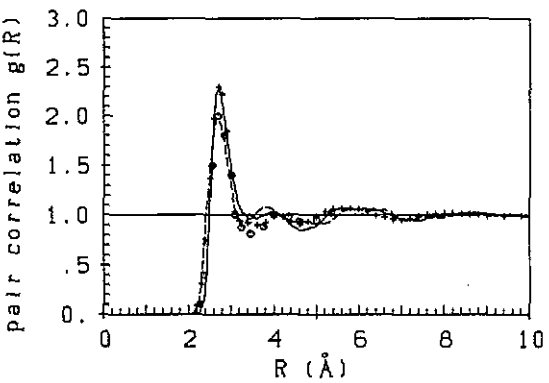

Figure 11. Pair correlation function $g(R)$ for liquid Ge at 1250 K, calculated using a pair-potential simulation for a $N = 1000$ atom ensemble (full line), and a simulation for a $N = 128$ atom ensemble using in addition three body forces (broken line). The crosses represent the experimental data by Waseda [53], open circles data by Bellisent–Funel and Bellisent [54].

7. Conclusion

Our aim was to construct norm-conserving 'soft-core' pseudopotentials with improved convergence properties of the plane-wave and perturbation expansions. The results presented in sections 3 to 6 show that this goal can be achieved, within the various extended norm-conserving pseudopotential schemes, by increasing the pseudopotential cut-off radii. There is always a certain trade-off between improved convergence

and a certain loss in transferability, but as long as for each angular momentum component the position of the maximum in the wave function is reproduced correctly, the pseudizing error is limited. Most of the results presented here refer to the Vanderbilt [20] pseudopotential, but we have shown that equivalent results may be obtained using the pseudopotential schemes of Rappe *et al* [28], Troullier and Martins [29] etc. The unifying feature is the kinetic energy of the valence pseudo-orbitals. As pointed out by Rappe *et al* [28], the kinetic energy contained in the Fourier components beyond a certain cut-off energy E_{cut} represents a reliable estimate of the total energy convergence. The total kinetic energy controls the convergence of the perturbation approach. Pseudopotentials having the same transferability will have similar expectation values for the kinetic energy and therefore nearly the same form of the screened pseudopotential matrix elements and effective pair interaction (figure 12). The potentials used are also very similar to those derived from optimized OPW pseudopotentials. The OPW pseudopotentials differ only in the large q-oscillations which cause their poor plane-wave convergence properties.

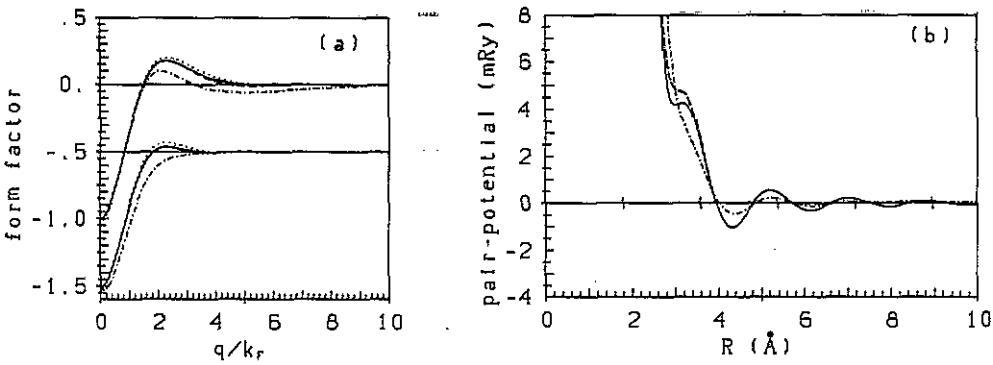

Figure 12. Screened pseudopotential form factor (left), and effective pair interaction (right) for Al, calculated using various pseudopotential schemes. Full curve VAN: R_{cl} = 1.8 au, broken curve TM : R_{cl} = 2.8 au and RRKJ: R_{cl} = 2.6 au, dotted curve BHS: R_{cl} = 1.6 au, dot-dashed curve OPW-pseudopotential [58]. The TM, RRKJ and BHS pseudopotentials are indistinguishable on the scale of the plot for the pair interaction.

With the optimized norm-conserving pseudopotential, we can now perform rapidly convergent total-energy calculations for the crystalline phases of a material and use pseudopotential perturbation theory to construct interatomic forces for the simulation of the liquid and amorphous phases, all using one and the same pseudopotential. This should allow us to make improved predictions for solid–liquid phase diagrams and to develop more efficient algorithms for *ab initio* molecular dynamics simulations.

References

[1] Hohenberg P and Kohn W 1964 *Phys. Rev.* B **136** 864
Kohn W and Sham L J 1965 *Phys. Rev.* A **140** 1133
[2] Car R and Parrinello 1985 *Phys. Rev. Lett.* **55** 2471
[3] Payne M C, Joannopoulos J D, Allan D C, Teter M P and Vanderbilt D H 1986 *Phys. Rev. Lett.* **56** 2656
[4] Teter M P, Payne M C and Allan D C 1989 *Phys. Rev.* B **40** 12255
[5] Nex C M M 1987 *J. Comput. Phys.* **70** 138

[6] Fermi E 1934 *Nuovo Cimento* **11** 15
[7] Hellmann H 1935 *Acta Phys.-Chim. USSR* **1** 913; Hellmann H 1938 *Acta Phys.-Chim. USSR* **4** 225
[8] Phillips J C and Kleinman L 1959 *Phys. Rev.* **116** 287
[9] Heine V and Weaire D 1970 *Solid State Physics* vol 24 (New York: Academic) p 247 ff
[10] Hafner J 1987 *From Hamiltonian to Phase Diagrams (Springer Series in Solid State Sciences 70)* (Berlin: Springer)
[11] Heine V and Hafner J 1990 *Many-Atom Interactions in Solids* ed R Nieminen, M J Manninen and M Puska (Berlin: Springer) p 33 ff
[12] Moriarty J A 1990 *Many-Atom Interactions in Solids* ed R Nieminen, M J Manninen and M Puska (Berlin: Springer) p 158 ff
[13] Cohen M H and Heine V 1962 *J. Physique Radium* **23**
[14] Harrison W A 1966 *Pseudopotentials in Theory of Metals* (New York: Benjamin)
[15] Hafner J 1975 *J. Phys. F: Met. Phys.* **5** 1243
[16] Joannopoulos J, Starkloff T and Kastner M 1977 *Phys. Rev. Lett.* **38** 660
[17] Hamann D R, Schlüter M and Chiang C 1979 *Phys. Rev. Lett.* **43** 1494
[18] Bachelet G B, Hamann D R and Schlüter M 1982 *Phys. Rev.* B **26** 4199
[19] Kerker G P 1980 *J. Phys. C.: Solid State Phys.* **13** L189
[20] Vanderbilt D 1985 *Phys. Rev.* B**32** 8412
[21] Shaw R W and Harrison W A 1967 *Phys. Rev.* **163** 604
[22] Topp W C and Hopfield J J 1974 *Phys. Rev.* B **7** 1295
[23] Hamann D R 1989 *Phys. Rev.* B **40** 2980
[24] Shirley E L, Allan D C, Martin R M, Joannopoulos J D 1989 *Phys. Rev.* B **40** 3652
[25] Devreese J T and Brosens F 1985 *Electronic Structure, Dynamics and Quantum Structural Properties of Condensed Matter* ed J T Devreese and P Van Camp (New York: Plenum)
[26] Redondo A, Godard W A and McGill T C 1979 *Phys. Rev.* B **15** 5038
[27] Christiansen P A, Lee Y S and Pitzer K S 1979 *J. Chem. Phys.* **71** 4445
[28] Rappe A M, Rabe K M, Kaxiras E and Joannopoulos J D 1990 *Phys. Rev.* B **41** 1227
[29] Troullier N and Martins J L 1991 *Phys. Rev.* B **43** 1993
[30] Vanderbilt D 1990 *Phys. Rev.* B **41** 7892
[31] Kleinman L and Bylander D M 1982 *Phys. Rev. Lett.* **48** 1425; *Phys. Rev.* B **41** 7892
[32] Laasonen K, Car R, Lee C, Vanderbilt D 1991 *Phys. Rev.* B **43** 6796
[33] Monkhorst J H and Pack J D 1976 *Phys. Rev.* B **13** 5188
[34] Ceperley D M and Alder B J 1980 *Phys. Rev. Lett.* **45** 566
[35] Lam P K and Cohen M L 1981 *Phys. Rev.* B **24** 4224
[36] Stedman R and Nilsson G 1966 *Phys. Rev.* **145** 492
[37] Nielsen O and Martin R M 1985 *Electronic Structure, Dynamics and Quantum Structural Properties of Condensed Matter* ed J T Devreese and P Van Camp (New York: Plenum)
[38] Lloyd P and Sholl C A 1968 *J. Phys. C: Solid State Phys.* **1** 1620
[39] McLaren R E 1976 *J. Phys. F: Met. Phys.* **6** 767
[40] Brovman E G, Kagan Y U and Holas A 1972 *Sov. Phys.-JETP* **34** 1300; **35** 783
[41] Hammerberg J and Ashcroft N W 1974 *Phys. Rev.* B **9** 409
[42] Kagan Y U, Pushkarev V V and Holas A 1977 *Sov. Phys.-JETP* **46** 511
[43] Hedin L and Lundquist B I 1969 *Solid State Physics* vol 23 (New York: Academic) pp 1
[44] Taylor R 1978 *J. Phys. F: Met. Phys.* **8** 1699
[45] Ichimaru S and Utsumi K 1981 *Phys. Rev.* B **24** 7385
[46] Bertoni C M, Bortolani V, Calandra C and Nizolli F 1984 *J. Phys. F: Met. Phys.* **4** 19
[47] Bertoni C M, Bisi O, Calandra C and Nizolli F 1975 *J. Phys. F: Met. Phys.* **5** 419
[48] Kagan Yu and Brovman E G 1974 *Dynamical Properties of Solids* vol 1, ed A A Maradudin and G K Horton (Amsterdam: North-Holland)
[49] Kresse G, Hafner J and Needs R J 1992 to be published
[50] Hafner J and Heine V 1983 *J. Phys. F: Met. Phys.* **13** 2479
[51] Hafner J and Heine V 1986 *J. Phys. F: Met. Phys.* **16** 1429
[52] Hafner J and Kahl G 1984 *J. Phys. F: Met. Phys.* **14** 2259
[53] Waseda Y 1981 *The Structure of Non-Crystalline Materials—Liquids and Amorphous Solids* (New York: McGraw-Hill)
[54] Bellisent-Funel M C and Bellisent R 1984 *J. Non-Cryst. Solids* **65** 383
[55] Hafner J 1989 *Phys. Rev. Lett.* **62** 784
[56] Hafner J 1990 *J. Phys.: Condens. Matter* **2** 1271

[57] Jank W and Hafner J 1990 *Phys. Rev.* B **41** 1497; 1990 *Phys. Rev.* B **42** 6296
[58] Jank W and Hafner J 1990 *Phys. Rev.* B **42** 11530
[59] Jank W and Hafner J 1992 *Phys. Rev.* B **45** 2739
[60] Stich I, Car R and Parrinello M 1989 *Phys. Rev. Lett.* **63** 2240
[61] Li X P, Allen P B, Car R, Parrinello M and Broughton J Q 1990 *Phys. Rev.* B **41** 3260
[62] Chang K J and Cohen M L 1986 *Phys. Rev.* B **34** 8581
[63] Kresse G and Hafner J 1992 to be published